Pion Showers in the CALICE AHCAL Prototype

The CALICE Collaboration *

February 22, 2011

In this note we present results from the data collected with the CALICE Analogue Hadronic Calorimeter (AHCAL) during the 2007 test beam at the CERN SPS. The data analyzed correspond to events collected using negative pion beams in the energy range 8 - 80 GeV. Detailed investigations of the shower properties in pion beam data are described and compared with results obtained with Geant 4 based Monte Carlo simulations. This is possible due to the high granularity of the scintillator-steel AHCAL prototype. The pion interaction length in the material mix of the AHCAL has been compared between simulations with several Geant 4 physics lists and measured data at different beam energies. A comparison between data and simulation in the longitudinal shower shape and the energy density is presented and the differences found are discussed.

*Author: Alexander Kaplan, Universität Heidelberg

Contents

1 Introduction **3**

2 Experimental setup **3**
2.1 The AHCAL Prototype 3
2.2 Setup at the CERN SPS H6 Test Beam 3

3 Calibration and Event Selection **4**
3.1 Calibration 4
3.2 Event Selection 5
3.3 The Primary Track Finder Algorithm 7

4 Simulation **7**
4.1 AHCAL Digitization 8
4.2 Physics Lists 8
4.3 Energy Decomposition 9

5 Results **12**
5.1 Total visible energy 12
5.2 First hard interaction 12
5.3 Longitudinal Shower Profiles 13

6 Summary and Conclusions **15**

A Additional Simulations **18**

B Nuclear Interaction Length for Pions from true MC **20**

C Software Versions and Calibration Constants **22**

1 Introduction

Measurements at the planned e^+e^- International Linear Collider (ILC) require a very high precision in energy - roughly a factor two better than what was achieved by detectors so far. One way to achieve the aimed jet energy resolution of $\sigma_E/E \approx 3-4\%$ is the Particle Flow approach [1, 2, 3]. Particles in a jet are measured depending on their nature in the detector providing the best energy resolution. For charged particles the tracker is used, for photons the electromagnetic calorimeter and for neutral hadrons the combined electromagnetic and hadronic calorimeter. In order to be able to distinguish single particles in the detector system and to minimize confusion in the assignment of energy very highly granular calorimeters are necessary. The optimization of calorimeter designs heavily depends on Monte Carlo simulations which have to be validated against real data.

The CALICE collaboration developed several calorimeter prototypes using different techniques proposed for calorimeters at a future e^+e^- collider. In a test beam program in 2006 and 2007 at the CERN SPS H6 beam line data was taken in a combined calorimeter setup.

In this note results from data taken with the CALICE analogue hadronic calorimeter prototype (AHCAL) are presented. The prototype and the combined test beam setup are described in section 2. Section 3 gives an overview of the data set investigated and the cuts applied to select events of interest. An algorithm to find the starting point of the hadronic shower is discussed. The tools used for the comparison of data and Monte Carlo simulation including a brief discussion of the Geant 4 [4] physics lists studied and a method used for the decomposition of deposited energy are introduced in 4. In section 5 the distribution of the initial point of the shower and longitudinal profiles are compared between data and simulation.

2 Experimental setup

The data investigated in this note have been obtained during a three-month test beam campaign at CERN in 2007. In this section we briefly introduce the AHCAL prototype and the test beam setup.

2.1 The AHCAL Prototype

The CALICE AHCAL prototype is a 1 m^3 sandwich calorimeter with 2 cm thick steel absorber plates and 38 active layers using 0.5 cm thick plastic scintillator tiles with varying areas of 3×3 cm^2 in the core up to 12×12 cm^2 in the outer part. The 7608 tiles are read out with Silicon Photomultipliers [5] via wave length shifting fibers. More details on the calorimeter and its commissioning can be found in [6].

2.2 Setup at the CERN SPS H6 Test Beam

The combined CALICE setup consisted of the Si-W electromagnetic calorimeter (ECAL), the scintillator-steel AHCAL and the scintillator-steel tail-catcher and muon-tracker (TCMT). The setup is sketched in Fig. 1. The trigger for the experiment is provided by a coincident signal from two 10×10 cm^2 plastic scintillators (Sc1 and Sc3 in the figure). Multi-particle events can be rejected offline using data from a 20×20 cm^2 multiplicity scintillator counter (Sc2) or from a 1×1 m^2 beam halo veto (Veto in the figure) with a central opening 20×20 cm^2 along the beam line. Separation of electrons and pions is performed with a Čerenkov counter upstream the setup, and muons are tagged by a 1×1 m^2 muon wall (Mc1) in the rear of the detectors. A more detailed description of the setup is available in [7].

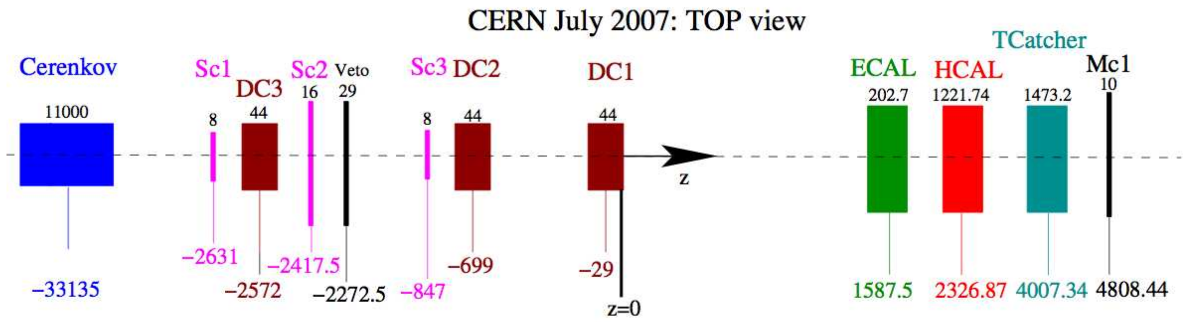

Figure 1: Setup during the 2007 data taking at CERN SPS H6 test beam site.

3 Calibration and Event Selection

3.1 Calibration

The equalization and calibration of calorimeter cell response including correction for temperature effects is performed with the CALICE software v03-00 [1] and according to the procedure described in [8]. The calibration chain can be summarized in the following steps:

- equalization of all cell responses
- correction of the non-linear SiPM response
- calibration with electromagnetic showers from test beam facilities

The factors for the equalization of cell response are obtained from muon runs acquired at CERN. The same equalization factors and SiPM response correction curves are applied to data and digitized Monte Carlo simulations (MC).

Calibration Uncertainties

The largest contribution to the calibration uncertainties is from the extraction of the MIP values used for the cell equalization and is in the order of 3%. This is an uncertainty on the energy scale and does not depend on the energy density. The value of 3% also includes the uncertainty on corrected short term temperature variations. Uncertainties on the SiPM non-linearity and the saturation point are instead energy density dependent. Their effect is negligible at low energies and becomes relevant, i.e. comparable to the MIP uncertainty, only for energies larger than 30 GeV.

Due to the complexity of the error propagation for these non-linear effects they are not included in the present note. A more careful study on the effect of calibration uncertainties is ongoing and the results will follow as an update to this note.

[1] A custom installation equivalent to v03-00 has been used - cf. appendix C

3.2 Event Selection

In this study pion events are selected using the standard trigger coincidence between the two trigger scintillators Sc1 and Sc2 (cf. section 2.2). Furthermore, pion showers are selected which had a first hard interaction in the ten layers of the AHCAL after the first one (layers number 2–11). The determination of the first hard interaction is performed using an algorithm called Primary Track Finder (PTF). The details of the algorithm will be discussed in detail in section 3.3. Events in which the shower starts in the first AHCAL layer are excluded to minimize possible systematic effects introduced by this algorithm. The purpose of the limit on the shower starting point to be in layers 2–11 is to minimize energy leakage from the AHCAL.

The requirement on the PTF to find the first hard interaction in the AHCAL automatically includes the rejection of muon events and leakage by electrons showering in the ECAL. Also empty events caused by fake triggers and multi-particle events are rejected.

Table 1 shows the selection of runs chosen for this analysis. For all energies at least 100k events have been recorded. At lower energies the amount of electrons in the beam is higher than at high energies. This reduces the overall pion statistics in the low energy runs.

Fig. 2 shows the reconstructed energy in all three CALICE calorimeters before and after applying the event selection requirements described above. After event selection, the energy distribution in the ECAL is consistent with that of a minimum ionizing particle. A large fraction of the pion energy is contained in the AHCAL, leading to the expected Gaussian distribution for the bulk of the data. A small tail is still present in the AHCAL energy distribution due to leakage to the TCMT. No further effort is made to select showers contained in the AHCAL in order not to bias the longitudinal shower profiles to a particular type of events. The bottom row shows the correlation between the energy deposited in the TCMT and the sum of energy deposited in the ECAL and the AHCAL. A peak around 1-2 GeV energy deposited in the ECAL and AHCAL is clearly visible before applying event selection requirements. This peak is due to muons and pions traversing the AHCAL without interacting and it is removed by the event selection requirements.

Run	Energy	Particle	Tot. ev.	Ev. after cuts	Efficiency
330334	8 GeV	π^-	105773	14494	13.7 %
330332	10 GeV	π^-	178504	26414	14.8 %
330330	12 GeV	π^-	261601	45113	17.2 %
330328	15 GeV	π^-	179131	36677	20.5 %
330327	18 GeV	π^-	178369	37662	21.1 %
330326	20 GeV	π^-	180279	38764	21.5 %
330325	25 GeV	π^-	177620	38492	21.7 %
330960	35 GeV	π^-	182907	34768	19.0 %
330961	45 GeV	π^-	174589	39074	22.4 %
330962	80 GeV	π^-	179777	40325	22.4 %

Table 1: Set of runs investigated in this note. The shower is required to start in the front part of the AHCAL. The number of events after this cut is given in column five and as a relative value in the last column.

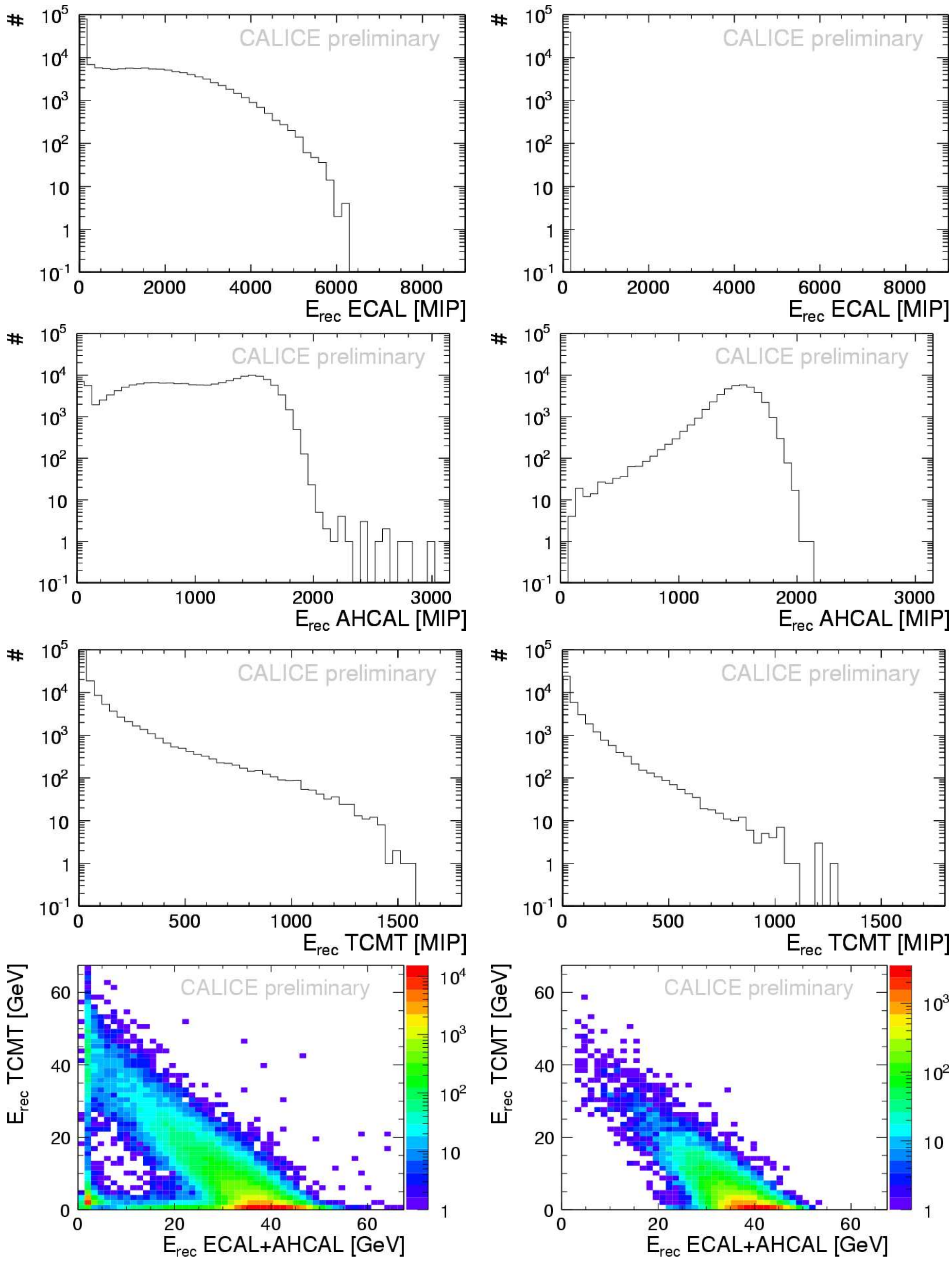

Figure 2: Distributions of reconstructed energy from 45 GeV pion showers in all three CALICE calorimeters before (left) and after (right) applying the event selection. In the bottom plots the correlation between the energy deposited in the TCMT and the sum of the energy deposited in the ECAL and AHCAL in GeV is shown.

3.3 The Primary Track Finder Algorithm

The Primary Track Finder algorithm (PTF) has been developed by M. Chadeeva [9]. Its purpose is to find the track corresponding to a primary particle entering the combined CALICE detector setup up to the starting point of its shower.

The starting layer is found using the accumulated average energy deposited,

$$A_i = \sum_{k=0}^{i} E_k/(i+1). \tag{1}$$

E_k being the energy deposited in layer k of the AHCAL.

The layer i where an hadronic shower starts is then defined as the first layer for which any of the following two criteria is fulfilled:

- $(A_i + A_{i+1}) > 6.5$ MIP and $N_i^{hit} + N_{i+1}^{hit} > 8$
- $E_{i+1} > E_{thr}$

where N_i^{hit} is the number of hits in layer i. The energy threshold E_{thr} expressed in units of MIP is heavily dependent on the beam energy. In the latest official version of the PTF this parameter is fixed for all events in one run, with a default value of 25 MIP. For this analysis a modified version of the PTF is used, with a threshold varying as a function of the energy deposited in the calorimeter system (sum of ECAL, AHCAL and TCMT). The information of the beam energy is not used by the algorithm. The energy dependence of the threshold value is parametrized by a first order polynomial. It is 14.5 MIP at 8 GeV and 32 MIP at 80 GeV energy deposited in the calorimeters.

Systematic uncertainty of the PTF algorithm

In order to evaluate systematic effects due to the PTF algorithm, the algorithm-determined layer of the first hard interaction is compared with the true point of first hadronic interaction in the Mokka [10] simulation. If this point is either inside an active AHCAL layer or in the absorber plate just before it, that layer is assumed to be the true starting point.

Fig. 3 Shows the performance of the PTF for an 80 GeV π^- run simulated using the QGSP_BERT physics list.

The performance of the PTF is dependent on the beam energy and the physics list used. For all physics lists and all energies for 74% (84%) of the events there is an agreement of better than ± 1 (± 2) layers between the first interaction layer found by PTF and the MC truth. Averaged over all energies and all physics lists, there is a systematic shift of -0.2 layers and a correlation of 85.8%. Further tuning might improve the quality of the PTF.

4 Simulation

The simulation of the entire setup is performed using the program Mokka version 7.02 [10]. Mokka is a Geant 4 based application able to simulate full ILC detector geometries as well as the 2007 CERN test beam setup. The geometry and materials used in the simulation are given in [7]. The simulated events from Mokka were passed through the CALICE digitization chain v03.01. The digitization includes emulation of light leakage across calorimeter cells and saturation effects in the AHCAL.

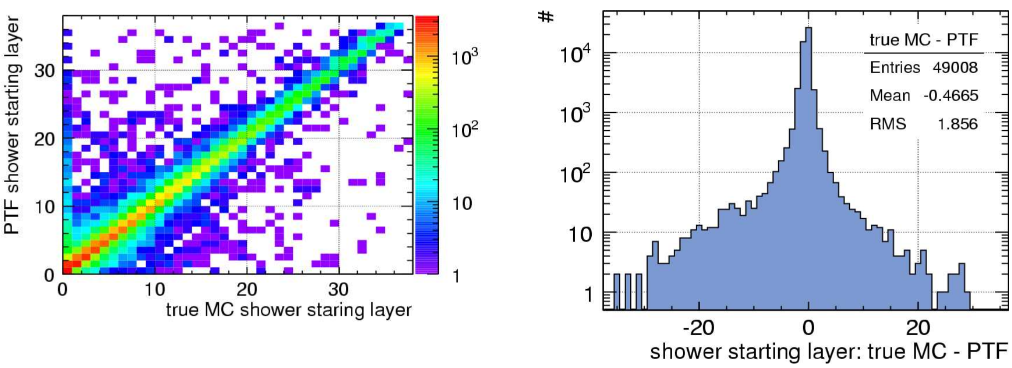

(a) (b)

Figure 3: Performance of the Primary Track Finder (PTF) compared to MC true using the QGSP_BERT physics list simulating an 80 GeV π^- beam. The correlation between the PTF and the true MC shower starting layer (a) is 97%. The average difference between the shower starting layer found by the PTF and the true one (b) is 0.5 AHCAL layers.

4.1 AHCAL Digitization

In Mokka the AHCAL detector is simulated with 1×1 cm^2 scintillator tiles. In the digitization these cells are then ganged to 3×3, 6×6 and 12×12 cm^2 cells according to the true geometry of the AHCAL prototype. As next step in the digitization, detector effects such as light leakage between tiles and non-linearity effects of the photo-detectors are simulated. For the current studies a light leakage factor of 10% between calorimeter cells is assumed. Non-linearity effects are simulated (and corrected during the reconstruction step) according to individual measurements for each calorimeter cell. More details on the digitization and the simulated detector effects can be found in [11].

4.2 Physics Lists

For the simulation of hadronic showers several models exists which partially differ in their predictions. The Monte Carlo simulation framework Geant 4 implements different models [12] valid in certain energy ranges and combines them in so called physics lists:

QGS The Quark-Gluon-String model is used to simulate the interactions of protons, neutrons, pions and kaons with nuclei in the energy range from 10 GeV to 50 TeV. It needs other models (e.g. Pre-Compound) to de-excite and fragment the residual nuclei.

FTF In the Fritiof model string formation is performed via scattering of projectiles on nucleons. It is valid for energies > 4 GeV.

LEP & HEP are the low energy parameterized (LEP) and high energy parameterized (HEP) models which have their origins in the GHEISHA hadronic package. They depend on parameterized fits to measured data and are no detailed theory driven hadronic models.

Physics List	Model content (for $\pi^{\pm}$)
`LHEP`	`LEP` (0–55 GeV); `HEP` (>25 GeV)
`QGSP_BERT`	Bertini (0–9.9 GeV); `LEP` (9.5–25 GeV); `QGSP` (>12 GeV)
`FTF_BIC`	`BIC` (0–5 GeV); `FTFB` (>4 GeV)
`CHIPS`	applied over full energy range

Table 2: The table shows the physics models invoked for pion inelastic interactions in each physics list. Where ranges overlap, `GEANT4` chooses randomly between models, with probabilities varying linearly with energy over the range of overlap.

Energy and momentum are only conserved on average, but not event by event. These models are outdated but are still commonly used in many Geant 4 physics lists for particles or energy ranges for which not better model exists.

Binary cascade This model is used for low energies (< 10 GeV). Nucleon-nucleon scattering is done by resonance formation and decay.

Bertini cascade This model includes intra-nuclear cascades followed by pre-compound and evaporation phases for the residual nucleus and is valid for low energies (< 10 GeV).

Pre-Compound model Theory driven model. It is used as back-end for other models to model pre-compound and evaporation phases of residual nuclei.

In the Geant 4 physics lists there are overlaps in the energy ranges the several models are applied. In these transition from one model to another model Geant 4 chooses randomly between the two models on an event-by-event basis. The following physics lists [13] were considered:

LHEP is a combination of LEP and HEP.

QGSP_BERT is a combination of the QGS model with the Pre-Compound model above 12 GeV, the Bertini cascade below 9.9 GeV and LEP parameterization between 9.5 GeV and 25 GeV.

FTF_BIC uses the Binary cascade for protons, neutrons, pions and kaons for energies below 5 GeV. For energies above 4 GeV the Fritiof model is used. The BIC model is again used for the re-scattering of secondaries in this case.

CHIPS The experimental Chiral Invariant Phase Space (CHIPS) physics list which simulates all elastic and inelastic hadron-nuclear reactions, photo/lepto-nuclear reactions, the stopping of hadrons and synchrotron radiation. For the simulation of events with this physics list the patched Geant 4.9.3.p01 version was used.

The physics content of these physics lists for pions is summarized in Table 2.

4.3 Energy Decomposition

Mokka allows to determine the energy deposited by a given particle type in a certain simulated material volume. However, this information is only available in the first stage of the simulation chain, still at the 1×1 cm^2 tile level, and it is lost in the first step of the digitization, i.e. the ganging. Due to the non-linear detector effects, threshold effects and non-Gaussian calibration smearing, data and simulation comparison can only be performed at the digitized MIP level. In the following we describe the method developed to retrieve single particle energy deposition in the scintillator (visible energy) event-by-event through the digitization chain - see also Fig. 4.

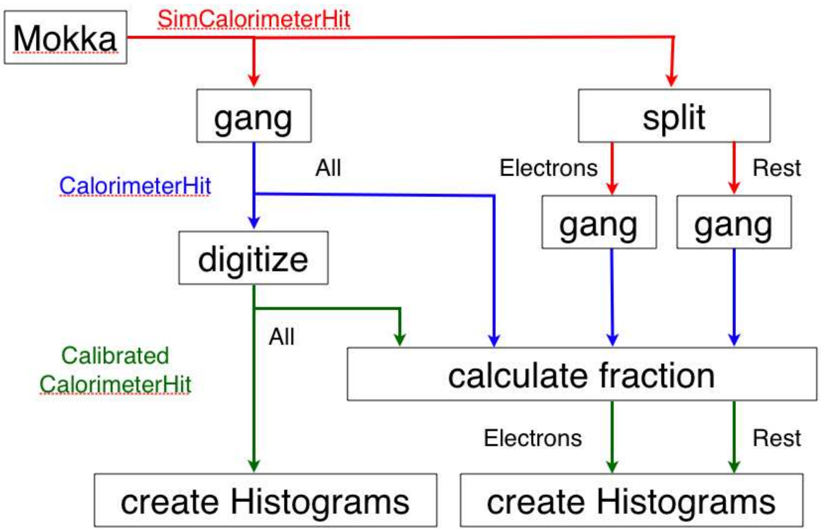

Figure 4: Flow chart of the developed technique to access the energy deposited by single particles in Mokka. For simplicity the process is only shown for one particle type (Electrons) and all other particles (Rest).

- A collection of visible energy is created for each particle type. The collections are filled event-by-event at the 1×1 cm^2 tile level.
- The 1×1 cm^2 hits divided in particle-type specific collections are then ganged, and new collections are created containing information at the real size tile level - the same way as for the hits not decomposed by particle type.
- For the merged hits the ratio between energy deposited by a certain particle type and the total energy are calculated. These ratios are used as weights to obtain, after the digitization steps, the fractions of particles of various type.
- The standard AHCAL digitization is applied to all hits, including a threshold cut of 0.5 MIP to reject noise.
- After digitization the total energy at the MIP scale is multiplied by the weights previously obtained to get the digitized fractional energy of each particle type.

The result of the visible energy decomposition is shown in Fig. 5 for 80 GeV pions. A difference of $\approx 7\%$ between the peak of the energy sum from data and the one from the FTF_BIC prediction (filled histogram) is visible. The observed difference is consistent with another independent investigation [14]. The other histograms in Fig. 5 are the distributions

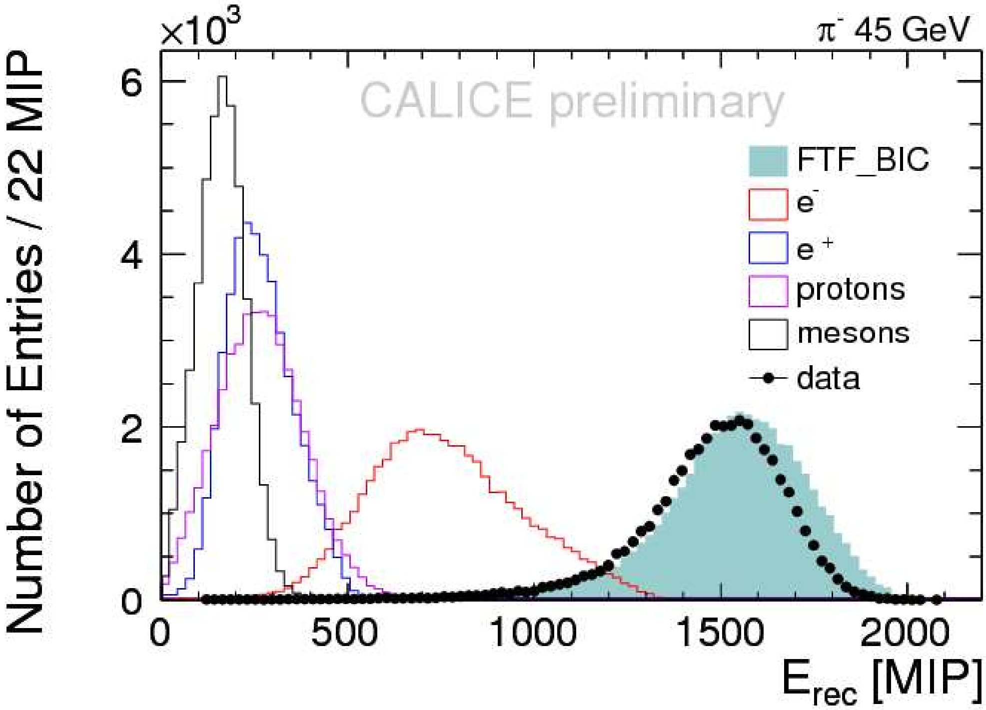

Figure 5: The breakdown of the reconstructed visible energy into the contributions from various particles in the shower: $e^{\pm}$, p, and mesons ($\pi^{\pm}$ and $K^{\pm}$).

of visible energy deposited by individual particle types, i.e. $e^{\pm}$, p, and mesons ($\pi^{\pm}$ and $K^{\pm}$). The information can be used to investigate disagreements between data and simulation in same observables to a deeper level, as it will be shown in the following.

5 Results

In this section we present the results of the comparison between data and simulations for various observables. We try to outline which physics list is closest to the data in the energy range covered by these studies. All results apply the calibration procedure and the event selection criteria described in section 3.

5.1 Total visible energy

The ratio between the reconstructed energy for the simulated and for the negative pion showers is shown in figure 6 at beam energies of 8, 18 and 80 GeV. The CHIPS physics list shows an energy independent overestimation of roughly 8%, while the response of the other physics lists varies. This overestimation is expected, since the low energy neutron cross-sections are not yet properly implemented in CHIPS [15]. LHEP predicts 9% too low energy deposition at 8 and 18 GeV (LEP parameterization) and 4% too low energy deposition at 80 GeV (HEP parameterization). The QGSP_BERT physics lists agrees with the data within the uncertainty at 8 and 18 GeV (Bertini Cascade and LEP), while at 80 GeV the QGS high energy model overestimates the energy by 6%. The FTF_BIC physics list behaves very similar: it underestimates the energy by 4% at 8 GeV (Binary cascade and FTF), agrees within the uncertainty at 18 GeV and gives 4% to high energy deposition at 80 GeV (at both higher energies FTF dominates the description of the first hard interaction).

5.2 First hard interaction

Exploiting the high granularity of the AHCAL, the position of the first hard interaction of hadrons in the calorimeter is determined. This information is used to deconvolute the true longitudinal development of the hadronic showers from the starting point. In figure 7(a) the shower profile from the calorimeter front face (filled histogram) and the one relative to the first interaction point (black line) are shown.

If the fluctuations of the shower starting position are removed the shower looks shorter and more similar to an electromagnetic one. As it will be discussed later in section 5.3, electromagnetic processes indeed dominate the shower shape.

From the distribution of the shower starting position one can directly extract the effective nuclear interaction length of pions in the material mix of the AHCAL. An example of the distribution and the applied exponential fit is shown in figure 7(b). This is a consistency check of the validity of the PTF algorithm applied on both data and MC. The effects introduced by the uncertainty of the PTF algorithm are largest in the first two and the last eight calorimeter layers. These layers are excluded from the fit. Figure 8 shows the values of the pion interaction length λ_{int}^{π} in cm extracted from the data and from the various physics lists.

The statistical error on λ_{int}^{π} extracted from the fits is below 1%. The uncertainty of the algorithm distorts the exponential form of the shower starting point distribution and translates into a systematic uncertainty on the interaction length extracted from the fits. This uncertainty is dependent on the physics list used and the beam energy. To estimate this

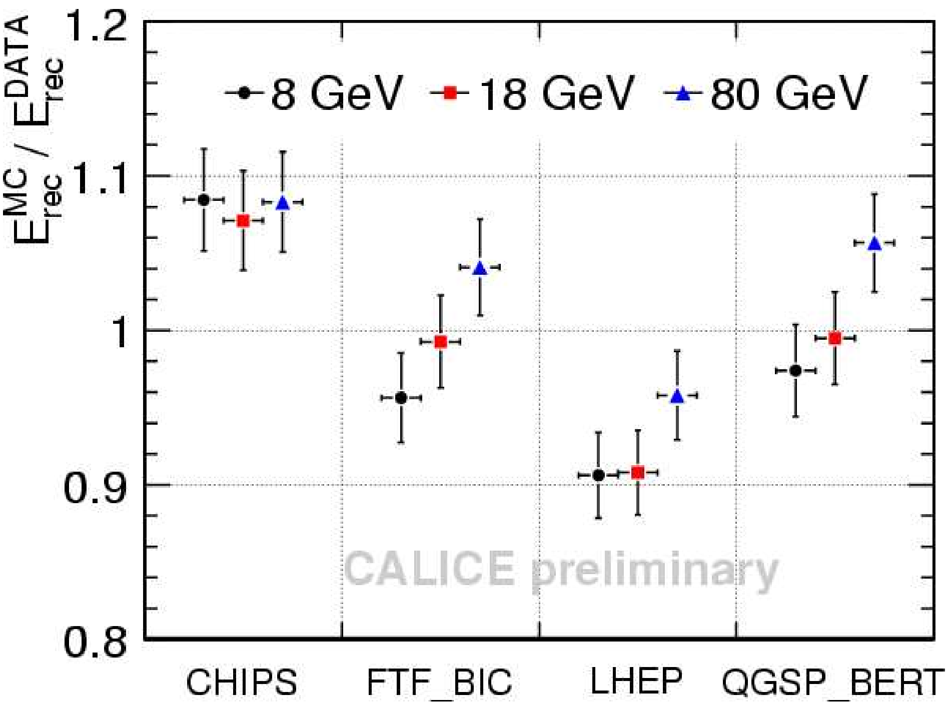

Figure 6: Ratio between the reconstructed energy in the AHCAL from simulation and from data for negative pion showers as a function of beam energy. All physics lists except CHIPS show an energy dependent behavior.

uncertainty two fits are performed, one to the true MC distribution and one to the distribution obtained determining the first interaction layer with the PTF algorithm. The RMS of the difference between the two fit values for each beam energy is used as uncertainty for the interaction length. The uncertainty varies from roughly 5% at 8 GeV to less than 1% at 80 GeV. In addition, a systematic increase of 4-5 cm is observed for all physics lists in the λ_{int}^{π} obtained using the algorithm with respect to the true MC one (c.f. Appendix B). The same systematic errors are assumed for the data.

Within uncertainties the fit yields the same effective nuclear interaction length, $\lambda_{int} \sim 30$ cm for all the physics lists which use the same pion cross section (all apart from LHEP which has a larger cross-section and a $\lambda_{int} \sim 26$ cm, and CHIPS which has a smaller cross-section and a $\lambda_{int} \sim 31$ cm). Data are found to be consistent with the majority of the models yielding a value of $\lambda_{int} \sim 29\pm1$ cm. The effect of the transition from QGS to LEP in the QGSP_BERT physics lists is visible below 25 GeV. Above 25 GeV, where the QGS model is applied, the QGSP_BERT physics lists agrees with the data.

5.3 Longitudinal Shower Profiles

Thanks to the very high granularity of the CALICE calorimeters, the longitudinal profile of hadronic showers can be investigated with an unprecedented accuracy. In particular, the true longitudinal development can be de-convolved from the distribution of the shower starting points. When measured from the position of the first hadronic interaction, as opposed to from the calorimeter front layer, hadronic showers are shorter and any layer-to-layer fluctuations

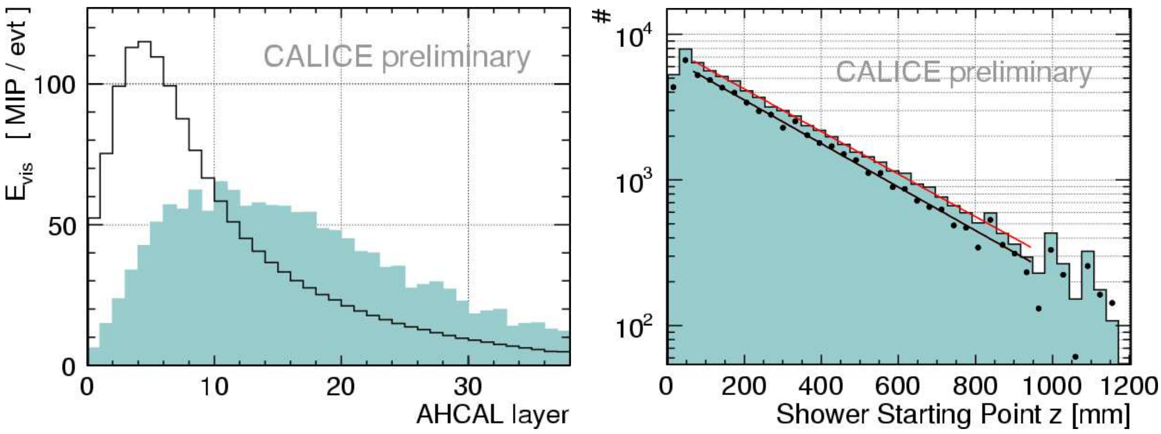

(a)

(b)

Figure 7: (a) Longitudinal profile for a 45 GeV π^- run relative to the calorimeter front (filled histogram) and relative to the first interaction (black line). (b) Distribution of shower start detected with the PTF in the GEANT4 simulation for the QGSP_BERT physics list (filled histogram) and 45 GeV pions data (filled circles).

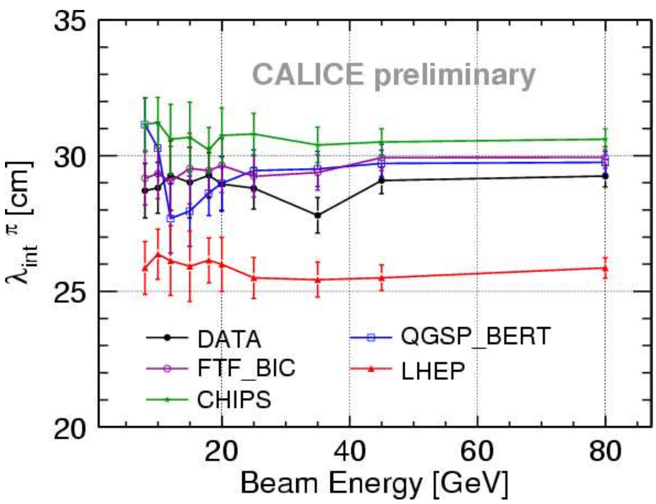

Figure 8: Extracted values for the interaction length in cm from data and MC models. The error bars shown are the uncertainty from the fitting added in quadrature with the uncertainty of the algorithm to determine the first interaction layer (see text). The 35 GeV run is currently under investigation.

introduced by calibration and dead channel effects are washed away.

The breakdown of the energy contribution from various particles in the shower ($e^{\pm}$,p, $\pi^{\pm}$, $\mu^{\pm}$) can be determined for the simulated events. This additional information helps to understand which physics processes contribute most in which phase of the shower development. This is clearly visible comparing the electron and positron contribution to the entire profile. The hadrons only contribute significantly in the very first layers after the first hard interaction.

In this analysis pion events collected at three different energies have been chosen to compare the longitudinal shower profile measured in data to that obtained from MC. The various MC models playing a role at low, medium and high energies are investigated.

Fig. 9 shows the longitudinal shower profiles for pions of 8, 18 and 80 GeV. The black points are data which are compared to the various MC models shown as filled histograms. The error bars show the effect due to the uncertainty in the determination of the first hard interaction only, and were estimated from comparison to profiles relative to the true first interaction layer in MC. The dominant systematic uncertainty from calibration is a 3% error on the energy scale. This would result in a coherent scaling of the whole spectrum and is therefore not shown here.

The position of the shower maximum is in general quite well simulated. All models except CHIPS tend to underestimate the tails of the showers seen in data.

At 8 GeV LHEP overestimates the deposited energy in the first layer. After the fifth layer it predicts to little energy. The QGSP_BERT physics lists agrees with the data within the uncertainty. The FTF_BIC simulation is similar to the one using QGSP_BERT. The predicted showera are slightly to short than in data. In layers 1-3 CHIPS agrees with the data, but the showers are too long.

All physics are close to data until approximately one λ_{int}^{π} after the first hard interaction at 18 GeV beam energy. Bigger differences become visible after this point for CHIPS (up to 30% overestimation) and LHEP (down to 30% too little energy deposition). The data are well described by QGSP_BERT, besides slightly too short showers. The performance of FTF_BIC is a little worse, but comparable to QGSP_BERT. Too much energy is deposited by CHIPS in the shower maximum and the showers are too long.

At 80 GeV LHEP simulates the tail of the shower profile quite well, but the energy deposition in the shower maximum is too low by almost 20%. The other three physics lists overestimate the energy in the shower maximum by $20 - 25\%$. The highest energy deposition is predicted by QGSP_BERT, followed by FTF_BIC. Both simulate too short showers. The longitudinal shower shape predicted by CHIPS at this energy is closer to data. Still theres is too much energy in the shower maximum and the showers are too long. Since the energy deposition in the shower maximum is dominated by electrons and positrons, the overshoot in the energy there predicted by QGSP_BERT, FTF_BIC and CHIPS could be a hint to a too high electromagnetic fraction at 80 GeV.

6 Summary and Conclusions

In this note several variables related to the shower physics have been investigated in order to compare Geant 4 models and to validate them against data from real pion showers in the AHCAL detector in the range from 8 - 80 GeV. Events have been simulated using several Geant 4.9.3 physics lists as well as the CHIPS physics lists from the patched version Geant 4.9.3.p01.

The calorimeter response predicted by four physics lists has been investigated and compared to data. The QGSP_BERT, FTF_BIC and LHEP physics lists show an energy dependent deviation from data. The CHIPS physics lists estimates roughly 8% to high response, but looks promising since it does not show a dependency on the beam energy. The overestimation of the response is expected by the developers due to the low energy neutron cross sections

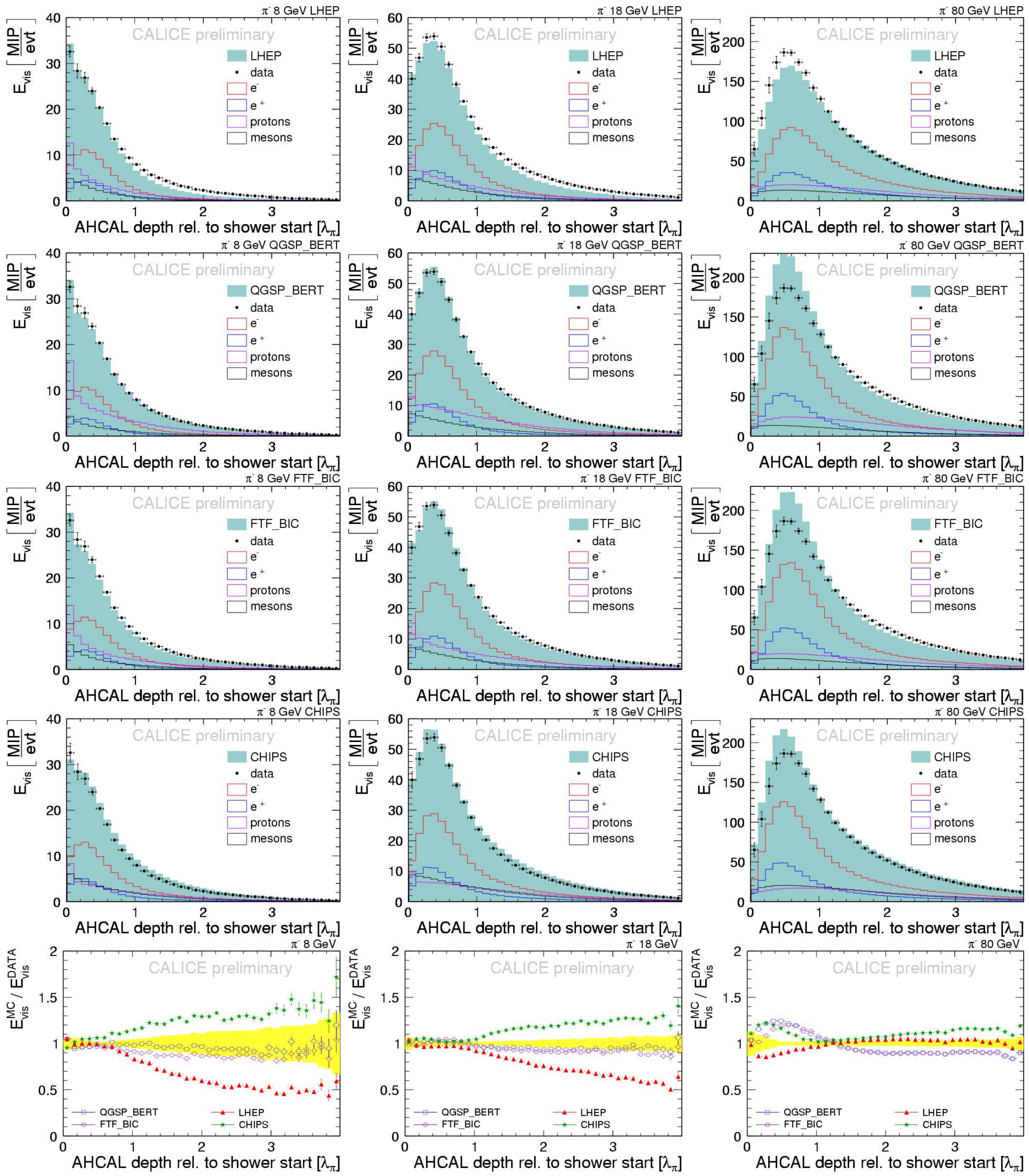

Figure 9: Longitudinal shower profile for 8, 18 and 80 GeV pions. The error bars include the statistical uncertainty and the uncertainty introduced by the determination of the first hard interaction. The breakdown of the energy contribution from various particles in the shower ($e^{\pm}$,p, $\pi^{\pm}$, $\mu^{\pm}$) is shown. The bottom row of plots shows the ratio of simulation and data.

not yet implemented properly.

The nuclear interaction length λ_{int}^{π} for pions in the AHCAL have been extracted from the distribution of the first hard interaction position found with the Primary Track Finder algorithm. The values for λ_{int}^{π} extracted from the Monte Carlo simulations have been compared to the ones for the data at different beam energies. This is a test of the pion cross sections implemented in the physics lists. Good agreement between the FTF_BIC physics list and data is found. LHEP simulates a higher cross section than the other physics lists which results in an too low interaction length compared to data. The application of the LEP model in the QGSP_BERT physics list at energies below 20 GeV is clearly visible. Above 20 GeV QGSP_BERT describes the DATA as well as FTF_BIC. For the CHIPS physics list a too high interaction length compared to data is found. This was expected by the developers due to the quasi-elastic and diffractive cross-sections used.

The last variable studied are highly granular longitudinal shower profiles relative to the position of the first hadronic interaction. The Mokka simulation allows to access the contribution of single particle species to the calorimeter hits which might give a hint for the reason of the disagreement between simulated and real showers. Profiles at three beam energies where different MC models in the physics lists come into play are presented. Showers in data are systematically longer than the predictions by QGSP_BERT, FTF_BIC and LHEP. Too long showers are found for the CHIPS and have been predicted by the developers. At high energies all physics list but LHEP simulate a too high energy deposition in the shower maximum.

The Primary Track Finder used for the studies in this note is still in development and results might further improve. The correct treatment of calibration uncertainties is still missing and will follow as an update to this note.

A Additional Simulations

More simulations with additional physics lists (all Geant 4.9.3) have been done and are presented in this appendix. Longitudinal profiles for 8, 18 and 25 GeV for the following physics lists are shown in fig. 10:

QGSP_FTFP_BERT This is a variant of the QGSP_BERT physics list where the LEP parameterization is replaced by the FTF model in the interval (6 GeV $< E <$ 25 GeV). The Bertini models overlaps with FTF in the range (6 GeV $< E <$ 8 GeV), while the QGS model overlaps with FTF in the range (12 GeV $< E <$ 25 GeV).

QGS(P)_BIC Combination of the QGS model at high energy with the Binary cascade model at low energy and the usual bridge between the two covered by LHEP. In the version with the Pre-Compound model turned on (QGSP_BIC) the BIC model is not used for pions (only for neutrons and protons).

FTFP_BERT_TRV Uses the Pre-compound model and the Bertini cascade for the low energy region. For the high energy region, the Fritiof model is used. FTFP_BERT_TRV is a variant of FTFP_BERT with the transition region between the BERT and the FTF model shifted from 4-5 GeV (default) to 6-8 GeV.

The physics content of these models for pions is summarized in Table 3.

Physics List	Model content (for $\pi^{\pm}$)
QGSP_FTFP_BERT	Bertini (0–8 GeV); FTFP (6–25 GeV); QGSP (>12 GeV)
QGS_BIC	BIC (0–1.3 GeV); LEP (1.2–25 GeV); QGSB (>12 GeV)
QGSP_BIC	LEP (<25 GeV); QGSP (>12 GeV)
FTFP_BERT_TRV	Bertini (0–8 GeV); FTFP (>6 GeV)

Table 3: The table shows the physics models invoked for pion inelastic interactions in each physics list. Where ranges overlap, GEANT4 chooses randomly between models, with probabilities varying linearly with energy over the range of overlap.

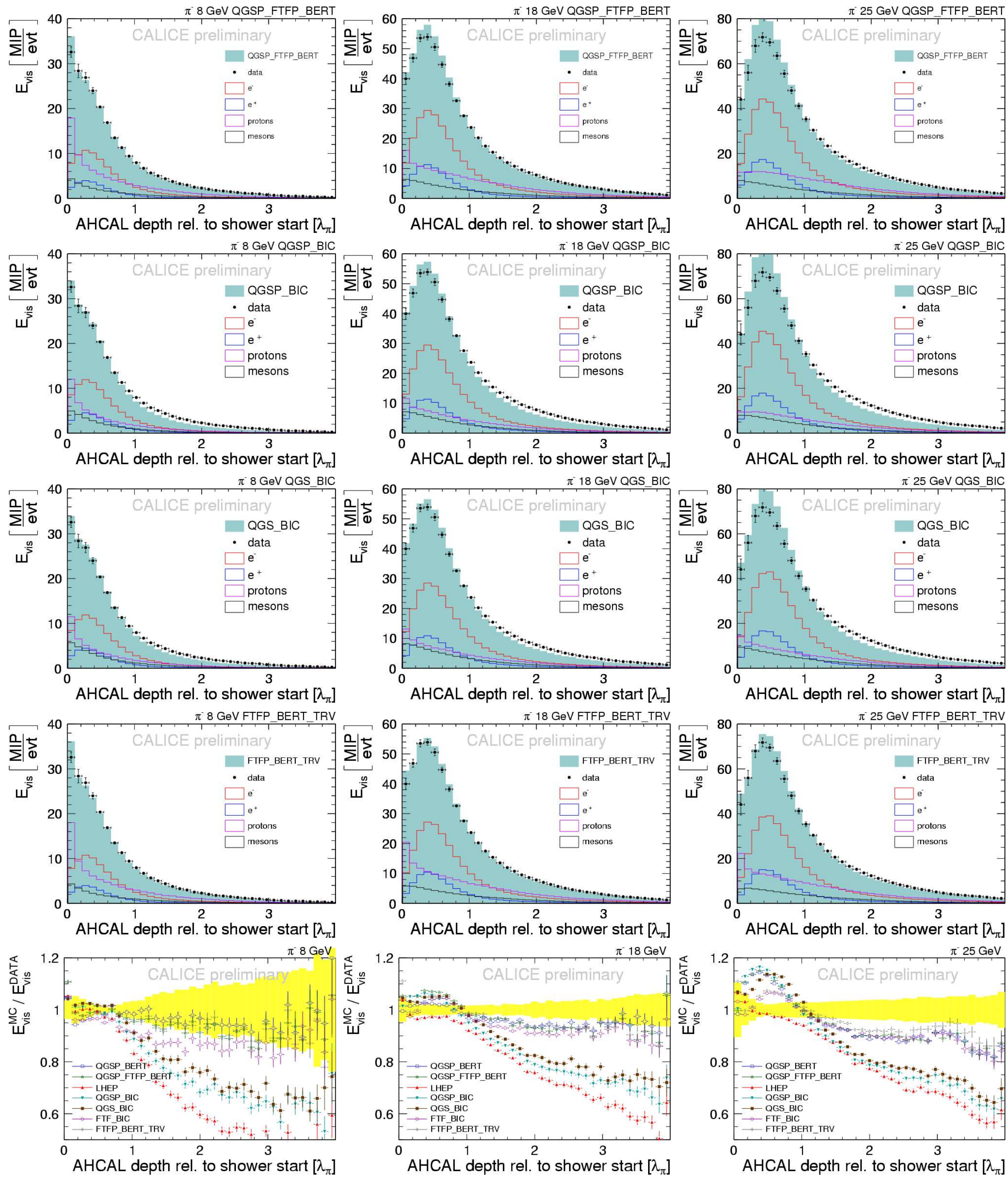

Figure 10: Longitudinal shower profile for 8, 18 and 25 GeV pions. The error bars include the statistical uncertainty and the uncertainty introduced by the PTF.

B Nuclear Interaction Length for Pions from true MC

To estimate the uncertainty on λ_{int}^{π} found with the PTF, also the true interaction length $\lambda_{int}^{\pi,true}$ using the real first interaction layer available in MC has been obtained. It has been extracted using the same procedure as described in section 5. The extracted values are shown in Fig. 11 for all physics lists (a), a zoomed picture is given in (b). All physics lists (excluding LHEP) use the same cross section for the pion interactions and thus the same interaction length within the uncertainty from the fit is found. Since no distortion of the exponential distribution for the shower starting layer due to the PTF is present, the absolute values of $\lambda_{int}^{\pi,true}$ are systematically smaller by 4-5 cm than the ones found by the PTF. The extracted values of the pion interaction length found by the PTF are shown in fig. 12.

The difference between the interaction length found using the true first interaction length and the one found using the PTF has been average over all physics lists. The RMS of this value is a measure for the uncertainty λ_{int}^{π} found with the PTF. In table 4 the mean shift and uncertainty for each energy point is summarized.

Beam Energy [GeV]	$\langle\lambda_{int}^{\pi}\rangle$ [mm]	$\langle\lambda_{int}^{\pi} - \lambda_{int}^{\pi,true}\rangle$ [mm]	RMS [mm]	$\Delta\left(\lambda_{int}^{\pi}\right)$
8	288	49	15	5 %
10	286	44	11	4 %
12	282	39	7	3 %
15	286	39	7	2 %
18	289	40	4	1 %
20	291	41	3	1 %
25	294	43	2	1 %
35	295	40	1	1 %
45	297	40	1	1 %
80	298	39	2	1 %

Table 4: Uncertainty introduced by the PTF on extracted interaction length averaged over all physics lists. The mean interaction length found by the PTF (1st column), the mean difference between the interaction length found using PTF and true MC (2nd column), the RMS of this value (3rd column), and the relative uncertainty on $\langle\lambda_{int}^{\pi}\rangle$ in percent (last column).

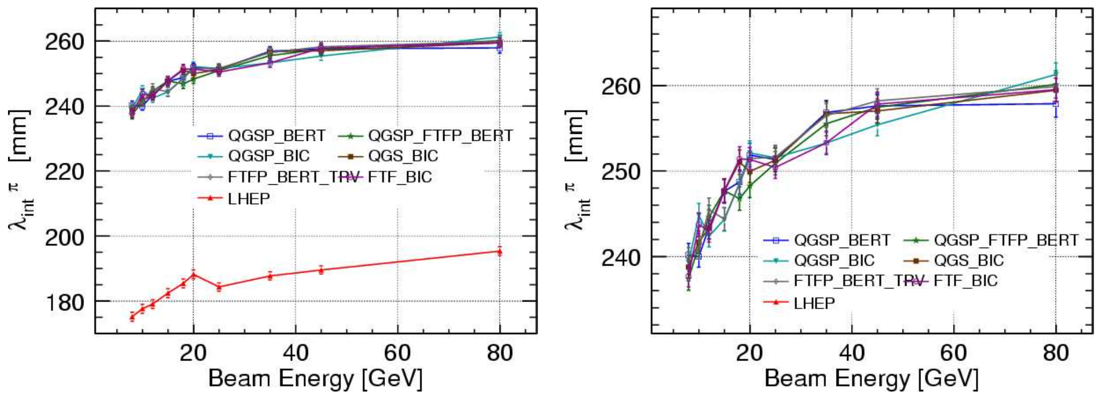

(a)

(b)

Figure 11: Pion Interaction length extracted using the true shower starting layer in Monte Carlo simulation for all physics lists (a) and zoomed in (b). Error bars shown are the fit uncertainty.

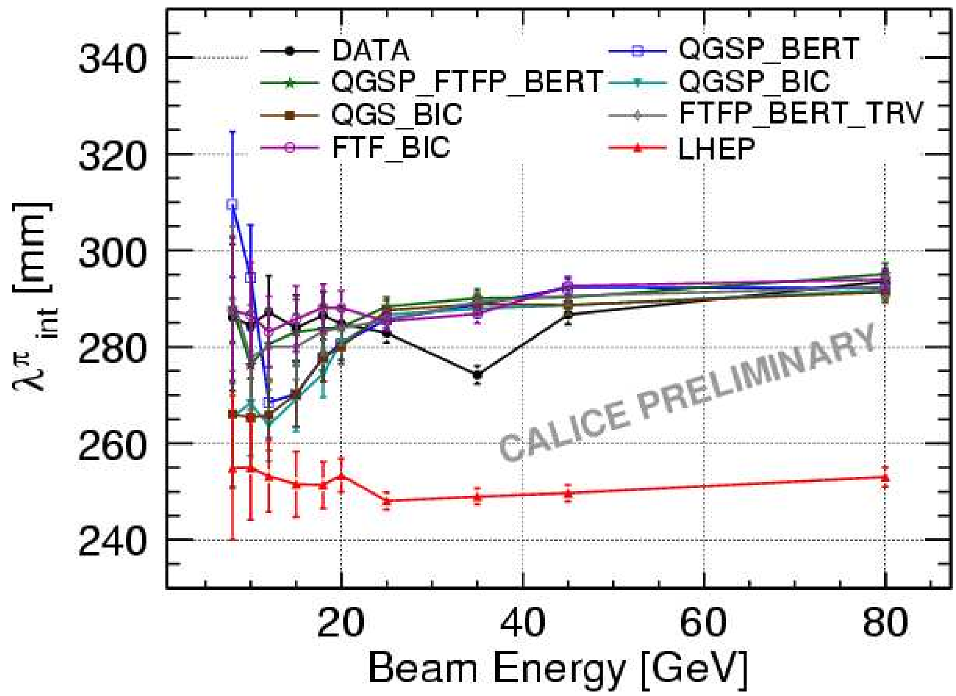

Figure 12: Extracted values for the interaction length in cm from data and MC models. Error shown are the uncertainty from the fitting added in quadrature with the uncertainty of the PTF to find the first interaction layer (see text). There is a problem with the 35 GeV run currently under investigation.

C Software Versions and Calibration Constants

The data and Monte Carlo simulations have been reconstructed and digitized using a custom software version since there was no official tagged version available at the time the data was processed. The software is nevertheless very close to the official tagged version v03-00 and should be equivalent.

Table 5 shows the database folder used during the reconstruction and digitization.

Collection Name	Data Base Path	Tag
`AhcMipConstants`	`/cd_calice/Hcal/mip_constants`	`ahc_mip_constants_002`
`AhcMipSlopes`	`/cd_calice/Hcal/mip_slopes`	`ahc_mip_slopes_002`
`AhcGainConstants`	`/cd_calice/Hcal/gain_constants`	`ahc_gain_constants_002`
`AhcGainSlopes`	`/cd_calice/Hcal/gain_slopes`	`ahc_gain_slopes_002`
`AhcInterConstants`	`/cd_calice/Hcal/ic_constants`	`ahc_ic_constants_002`
`AhcCellQuality`	`/cd_calice/Ahc/BadCellMap`	`ahc_bad_cell_map_001`
`AhcTempSensorCalib`	`/cd_calice/Hcal/tempSensors`	`ahc_tempSensors_001`
`AhcSroModMapping`	`/cd_calice_cernbeam/Hcal/AhcSroModMapping`	`ahc_AhcSroModMapping_001`
`AhcResponseCurve`	`/cd_calice/Ahc/ResponseCurve`	`ahc_response_curve_002`
`AhcResponseScaling`	`/cd_calice/Ahc/ResponseCurveScaling`	`ahc_response_curve_scaling_001`

Table 5: Database folders and versions tags of the calibration constants used.

References

[1] J.-C. Brient and H. Videau, "The calorimetry at the future e+ e- linear collider," in *Proceedings of APS / DPF / DPB Summer Study on the Future of Particle Physics (Snowmass 2001), Snowmass, Colorado*. July, 2001. arXiv:hep-ex/0202004.

[2] V. L. Morgunov, "Calorimetry design with energy-flow concept (imaging detector for high-energy physics)," in *Proceedings of the Tenth International Conference Pasadena, California, USA*. Mar., 2002.

[3] M. A. Thomson, "Particle Flow Calorimetry and the PandoraPFA Algorithm," *Nucl. Instrum. Meth.* **A611** (2009) 25–40, arXiv:0907.3577 [physics.ins-det].

[4] Geant4 working group, "GEANT4 - a simulaton toolkit." http://geant4.web.cern.ch/geant4/.

[5] G. Bondarenko *et al.*, "Limited Geiger-mode microcell silicon photodiode: New results," *Nucl. Instrum. Meth.* **A442** (2000) 187–192.

[6] C. Adloff *et al.*, "Construction and Commissioning of the CALICE Analog Hadron Calorimeter Prototype," *JINST* **5** (2010) P05004, arXiv:1003.2662 [physics.ins-det].

[7] A. Lucaci, "HCAL prototype in the test beam Mokka model." http://www.desy.de/~lucaci/Others/hcalTBeam.pdf.

[8] The CALICE collaboration, "Electron data with the CALICE tile AHCAL prototype at the CERN test-beam - Effect of temperature correction," *CAN* **014** (2008) .

[9] M. Chadeva , “Primary Track Finder Processor.” http://www-flc.desy.de/hcal/meetings/internal/minutes2009/090326-MC_hadrons2.pdf. Presentation given at weekly HCAL Meeting in FLC group at DESY.

[10] Mokka Working Group, “Mokka - a GEANT4 application to simulate the full ILD geometry.” http://polzope.in2p3.fr:8081/MOKKA.

[11] S. Richter, “Validation of the Calibration Procedure for a Highly Granular Calorimeter with Electromagnetic Processes,” Master’s thesis, University of Hamburg, 2008.

[12] Apostolakis, J. and others, “GEANT4 Physics Lists for HEP,” in *Nuclear Science Symposium Conference Record, 2008. NSS ’08. IEEE*, pp. 833 –836. Oct., 2008.

[13] Geant4 working group. http://www.geant4.org/geant4/support/proc_mod_catalog/physics_lists/referencePL.shtml. accessed February 17th 2010.

[14] B. Lutz, *Hadron Showers in a Highly Granular Calorimeter*. PhD thesis, University of Hamburg, 2010.

[15] M. Kosov, “CHIPS physics list in Geant4.” http://ilcagenda.linearcollider.org/getFile.py/access?contribId=126&sessionId=31&resId=0&materialId=slides&confId=4649.